Interaction of Hydrophobically End-Capped Poly(ethylene oxide) with Nonionic Surfactants in Aqueous Solution. Fluorescence and Light Scattering Studies

E. Alami, M. Almgren,* and W. Brown

Department of Physical Chemistry, University of Uppsala, Box 532, S-751 21 Uppsala, Sweden

Received December 11, 1995; Revised Manuscript Received April 18, 1996[⊗]

ABSTRACT: In ternary mixtures of an associative polymer (AP), hydrophobically end-capped poly(ethylene oxide), $C_{12}EO_{460}C_{12}$, and the nonionic surfactant, $C_{12}E_8$, hydrophobic microdomains are formed at much lower concentrations than the cac and cmc of the binary systems. Strong interactions promote formation of large networks and result in a substantial depression of the cloud point temperature, CPT (below that of the polymer and the surfactant), a decrease in the diffusion coefficient, and an increase in the solution viscosity. A more hydrophobic surfactant is more effective in forming these structures. At higher relative surfactant concentrations, however, the networks dissolve and the CPT increases. A second more hydrophobic AP added to a $C_{12}EO_{460}C_{12}$ solution does not change the solution structure in the same way. In mixtures of two APs, the CPT is found to lie in between those of the two polymers. The networks formed in this case are always smaller than those formed by either of the APs. Addition of an AP to a $C_{12}E_8$ solution slightly increases the total aggregation number of the hydrophobic domains above that of the pure surfactant aggregates. At concentrations where the surfactant structure dominates, the added polymer has been found to associate with the existing domains rather than forming new ones. The bulky hydrophobic groups of the AP in the ternary mixture effectively prevent the increase in N_{agg} with temperature observed in pure $C_{12}E_8$ systems and also in the presence of unmodified PEO.

Introduction

The present investigation of the interaction of a model associative polymer (AP), hydrophobically end-capped poly(ethylene oxide) ($M_w = 20\,800$), with nonionic surfactants of the ethylene oxide type and with an AP of lower molecular weight continues our study of the binary polymer system.[1] The main conclusions from the latter study were that most of the polymer molecules are free below $C_p < 10^{-3}$ g mL^{-1} or exist in the form of oligomeric aggregates. Hydrophobic micelle-like microdomains start to form above ca. 3×10^{-3} g mL^{-1} (static fluorescence) and have aggregation numbers around 15−30 end groups (dynamic fluorescence), independent of the polymer concentration. Larger multicentered clusters start to form at about $C_p > 7 \times 10^{-3}$ g mL^{-1} as shown by dynamic light scattering, and the overlap and bridging of these clusters are considered to be responsible for the abrupt viscosity increase starting at $C_p \approx 2 \times 10^{-2}$ g mL^{-1}. These observations are compatible with the results of fundamental studies performed on both binary (polymer−water) and ternary (polymer−water−surfactant) systems, employing techniques such as static and dynamic fluorescence,[1−6] light scattering,[1,7−9] surface tension,[7] NMR self-diffusion and relaxation,[9−13] ESR,[14] SAXS,[15] and SANS.[6]

The previous results are summarized in a schematic picture of the aggregation steps and aggregate structure (Figure 1). The absolute concentrations at the steps of the aggregation process vary dramatically with polymer mass and the hydrophilic−lipophilic balance.[6] In particular, for our AP having a rather high molecular weight, it is difficult to isolate a concentration region with only isolated "flower" micelles. The formation of clusters of micelles seems to start at concentrations close to the cmc.

Most studies of surfactants in ternary systems deal with anionic surfactants, usually SDS.[2,5,12−14,16−18] The general effects on addition of this surfactant are included in Figure 1. At low concentrations, below the cmc of the surfactant, SDS interacts mainly with the hydrophobic end groups of the polymer, resulting in a strengthening of the network and giving an increase in the viscosity of the solution.[5,13,16−18] At high surfactant concentrations, the end groups become solubilized and the network structure is destabilized. SDS micelles also interact with the oxyethylene main chain of the polymer.[2,5,12,13] Cationic surfactants, on the other hand, seem to interact only with the end groups of the polymer.[3,13] Unlike usual nonionic polymers,[19−20] the HEUR associative polymers have also been found to interact strongly with nonionic surfactants,[3] leading to a large increase in solution viscosity. The present study aims to further clarify the effect of the addition of nonionic surfactants on associative polymer association. For comparison, we have also investigated the effect of adding an AP with much lower molecular weight ($M_w = 6\,000$), although still much more hydrophilic than the surfactant.

Experimental Section

The model associative polymer (poly(ethylene didodecyl ether)) used in this study has the following simple chemical structure: ■−〰−■ where 〰 is a poly(ethylene oxide) chain (PEO; Hoechst) with a molecular weight of about 20 000 and ■ is a paraffinic chain with 12 carbon atoms. It is denoted $C_{12}EO_{460}C_{12}$. This sample was synthesized and purified by the method described in previous papers.[6,15]

The sample was characterized by size exclusion chromatography with THF as solvent. The chromatograms exhibit only one peak, corresponding to that of the unmodified PEO. The molar mass of PEO was $M_w = 20\,800$ with $M_w/M_n = 1.01$. $C_{12}EO_{460}C_{12}$ had $M_w = 20\,300$ with $M_w/M_n = 1.02$. The molar mass of $C_{12}EO_{136}C_{12}$ was $M_w = 6\,030$ with $M_w/M_n = 1.0$, and this polymer was prepared in the same manner as $C_{12}EO_{460}C_{12}$. The cloud point and the cac of $C_{12}EO_{136}C_{12}$ have been reported to be 13 °C and 10^{-4} g mL^{-1}, respectively.[6] The degree of

* To whom correspondence should be addressed.
[⊗] Abstract published in *Advance ACS Abstracts,* June 1, 1996.

S0024-9297(95)01816-X CCC: $12.00

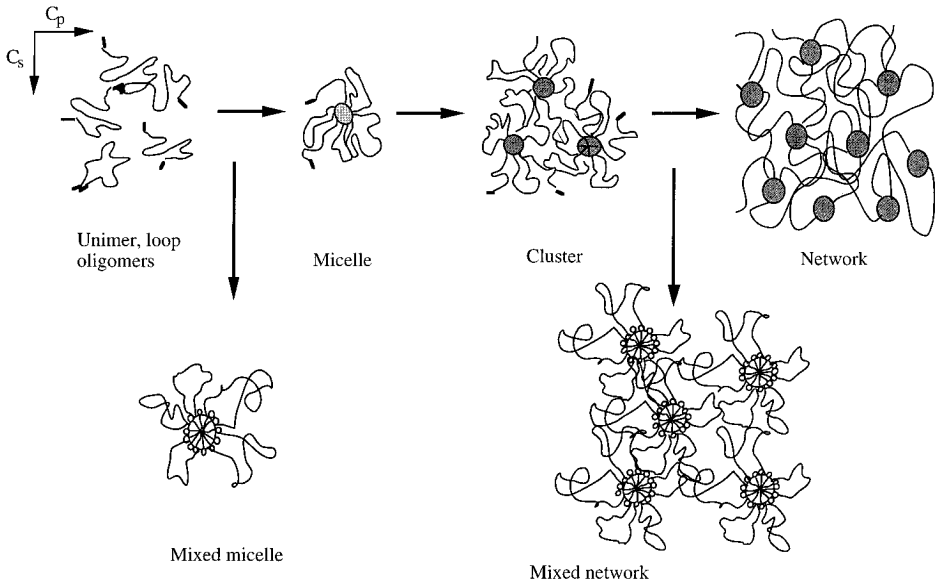

Figure 1. Schematic representation of the proposed AP aggregates at different polymer concentrations, with and without surfactant.

substitution of the hydroxyl groups was determined by ^{13}C, ^{1}H, and ^{2}H NMR and elemental analysis. The results were confirmed by a determination of the residual OH groups by UV spectroscopy after reaction of the naphthyl isocyanate group on the polymer. The degree of substitution was found to be 0.95 for $C_{12}EO_{460}C_{12}$ and 0.85 for $C_{12}EO_{136}C_{12}$.

$C_{12}E_8$ was obtained from Nikko Chemicals, Japan, and $C_{12}E_6$ from Bachem Feinkemikalien, Switzerland. The two samples were used without further purification. The cloud points of these two surfactants are 77 and 50 °C,[21] respectively, and their critical micelle concentrations are 71 and 68 μM, respectively.[22] $C_{12}E_{23}$, purchased from Sigma, was also used as received, and its cmc has previously been determined as 175 μM.[23] Pyrene (Py) and dimethylbenzophenone (DMBP), used in the fluorescence studies, were purchased from Aldrich.

Sample Preparation. The preparation of samples for fluorescence measurements has been described earlier.[5] To dissolve pyrene completely in the hydrophobic microdomains, the solutions were stirred at least overnight before measurement. The pyrene concentration used for the mixture with surfactant was $\leq 10^{-6}$ M. The DMBP concentration was chosen to be less than one DMBP molecule per micelle. The measurements were normally made on aerated samples. The lifetime τ_0 thus determined was affected by oxygen quenching, but it was shown that oxygen quenching had no effect on the determination of the aggregation number. For light scattering, all solutions were prepared in distilled water and filtered using 0.2 μm Millipore filters.

Steady-State Fluorescence. Pyrene I_1/I_3 ratios report changes in the environment of the probe.[24] The high sensitivity of this method facilitates determination of very low cac and cmc values. The equipment used for the steady-state fluorescence measurements was a SPEX Fluorolog 1680 combined with a SPEX Spectroscopy Laboratory Coordinator DM1B. The fluorescence spectra were measured between 350 and 500 nm with excitation wavelength at 320 nm.

Time-Resolved Fluorescence Quenching (TRFQ). Using dynamic fluorescence quenching, the micelle aggregation number, N_{agg}, can be obtained from analysis of the fluorescence decay curves determined using a single-photon-counting setup.[25] In this study, pyrene and dimethylbenzophenone (DMBP) were used as the fluorescent probe P and quencher Q, respectively. Two measurements were performed on each surfactant/polymer solution: one with only pyrene at very low concentration, [P] $\leq 10^{-6}$ M, yielding the probe fluorescence lifetime τ_0 in the micellar environment, and the second at the same low [P] and a quencher concentration [Q] comparable to the micelle concentration [M]. The determination of aggregation numbers from fluorescence quenching measurements is based on the Infelta-Tachiya equation for quenching in monodisperse micelles.[26,27] The fluorescence decay curves were shown to obey the equation

$$I(t) = I(0)\exp(-A_2 t - A_3[1 - \exp(-A_4 t)]) \qquad (1)$$

where $I(t)$ and $I(0)$ are the fluorescence intensities at time t and $t = 0$, respectively, following excitation. A_2, A_3, and A_4 are time-independent parameters that can be obtained, together with $I(0)$, by fitting eq 1 to the experimental data.

In the case where the distributions of probe and quencher over the micelles are frozen on the fluorescence time scale, the expressions for A_2, A_3, and A_4 are[28,29]

$$A_2 = k_0; \qquad A_3 = \frac{[Q]_m}{[M]}; \qquad A_4 = k_Q \qquad (2)$$

where $k_0 = 1/\tau_0$ is the fluorescence decay rate constant of the probe in the micelles without quencher and at low pyrene concentration (no excimer formation), [M] is the molar micelle concentration, $[Q]_m$ is the concentration of quencher in micelles, and k_Q is the pseudo-first-order rate constant for the intramicellar process. The lowest surfactant concentration, 2 mM, is already well above both the cac (ca. 0.75 mM) and the cmc (ca. 71 μM), and it can be assumed that all the polymer end groups are involved in the formation of mixed micelles and that the free surfactant concentration is negligible, so that the total aggregation number is given by

$$N_t = \frac{c_{eg} + c_s}{[M]} = \frac{A_3}{[Q]_m}(c_{eg} + c_s) \qquad (3)$$

where c_s is the total surfactant concentration and c_{eg} is the end-group molar concentration. The total aggregation number, N_t, is the aggregation number of the mixed micelle (end groups + surfactants) when the surfactant preferentially binds close to the end groups of the polymer and forms mixed-micellar type aggregates. The number of end groups of the polymer per micelle, N_{eg}, is given by

$$N_{eg} = c_{eg}/[M] \qquad (4)$$

At the lowest surfactant concentration used in this study, 2 mM, the distribution of the quencher between aggregates and the aqueous solution was considered. The distribution constant, K_D, defined by $[Q]_m/[Q]_{aq} = K_D[S]_m$, was estimated from UV-absorption measurements on the quencher DMBP in solutions and gave $K_D = 2.3 \times 10^3$ L mol^{-1} at 20 °C.

Dynamic Light Scattering (DLS). The scattering cells (10-mL cylindrical ampules) were immersed in a large-diameter thermostated bath of index-matching liquid (*trans-*

decalin). Polarized (VV) DLS measurements in the self-beating (homodyne) mode were performed using a frequency-stabilized Coherent Innova Ar ion laser operating at 488 nm with adjustable output power. A typical laser power was 500 mW for the polarized data at the higher concentrations. The incident light was vertically polarized with a Glan−Thompson polarizer, with extinction better than 10^{-6}.

The detector optics employed a 4-μm-diameter monomodal fiber coupled to an ITT FW130 photomultiplier, the output of which was digitized by an ALV-PM-PD amplifier−discriminator. The signal analyzer was an ALV-5000 digital multiple-τ correlator (Langen GmbH) with 288 exponentially spaced channels. It has a minimum real time sampling time of 0.2 μs and a maximum of about 100 s. The intensity autocorrelation function, $g^{(2)}(t)$, was measured at different angles. When not otherwise indicated, the temperature was 20 °C.

Data Analysis. The DLS data were analyzed by nonlinear regression procedures. The various models used in the fitting procedures are expressed with respect to $g^{(1)}(t)$, while the fitting was performed with respect to the measured $g^{(2)}(t)$, described as

$$g^{(2)}(t) - 1 = B[1 + \beta|g^{(1)}(t)|^2] \quad (5)$$

where β is a nonideality factor which accounts for the deviation from ideal correlation and B is a base line term. The autocorrelation function $g^{(1)}(t)$ can be written as the Laplace transform of the distribution of relaxation rate $G(\Gamma)$:

$$g^{(1)}(t) = \int_0^\infty G(\Gamma) \exp(-\Gamma t) d\Gamma \quad (6)$$

where Γ is the relaxation rate and t is the lag time. For relaxation times, τ, $g^{(1)}(t)$ is expressed here as

$$g^{(1)}(t) = \int_{-\infty}^{\infty} \tau A(\tau) \exp(-t/\tau) \, d \ln \tau \quad (7)$$

where $A(\tau) \equiv \Gamma G(\Gamma)$. $\tau A(\tau)$ was obtained by regularized inverse Laplace transformation (RILT) of the dynamic light scattering data using a constrained regularization calculation algorithm called REPES[30,31] as incorporated in the analysis package GENDIST. This algorithm directly minimizes the sum of the squared differences between experimental and calculated $g^{(2)}(t)$ functions. It allows the selection of a "smoothing parameter", *probability to reject*—the higher the probability to reject, the greater the smoothing. A value of 0.5 was normally chosen in the analysis.

Viscosimetry. The viscosity measurements were performed using an Ubbelohde capillary viscosimeter. The flow time for water at 25 °C was 43.8 s. The result of the measurements is expressed by the relative viscosity, $\eta_{rel} = t/t_0$, where t and t_0 are the flow times for mixed solution and solvent, respectively.

Results and Discussion

Solubility and Phase Diagram. (a) $C_{12}EO_{460}C_{12}$−$C_{12}E_8$ System. One important property of an associative polymer $C_{12}EO_{460}C_{12}$ in water solution is the separation into two phases above the cloud point temperature, a phenomenon which is well known for unmodified PEO as well as poly(ethylene oxide) surfactants (C_nE_m). Cloud point measurements were performed by visual observation in glass tubes. After heating the samples to above the clouding temperature, the cloud point was taken as the temperature at which the last visible sign of opalescence disappeared on cooling. Cloud point data for the polymer $C_{12}EO_{460}C_{12}$ are presented in Figure 2 as a function of concentration. The decrease of the cloud point, as compared to the unmodified homologue PEO, LCST (lower critical solution temperature) = 102 °C,[32] is due to the presence of the hydrophobic end groups.[6] The polymer and the surfactant $C_{12}E_8$ have cloud points in the same temperature range, LCST ≈ 75 °C.

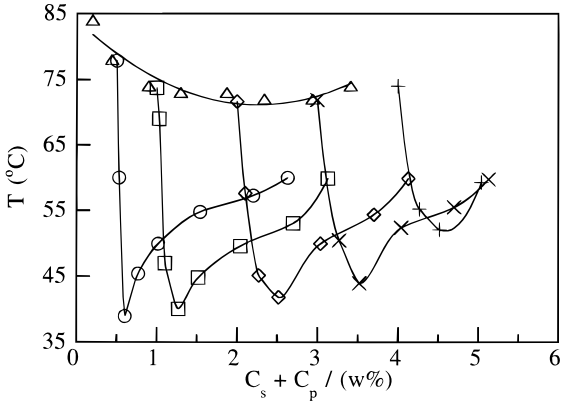

Figure 2. Cloud point temperature of aqueous solutions of the associative polymer $C_{12}EO_{460}C_{12}$ (Δ) and of mixtures with the surfactant ($C_{12}E_8$) at 0.5 (○), 1.0 (□), 2.0 (◇), 3.0 (×), and 4.0 (+) wt % polymer as a function of the total content (C_p + C_s).

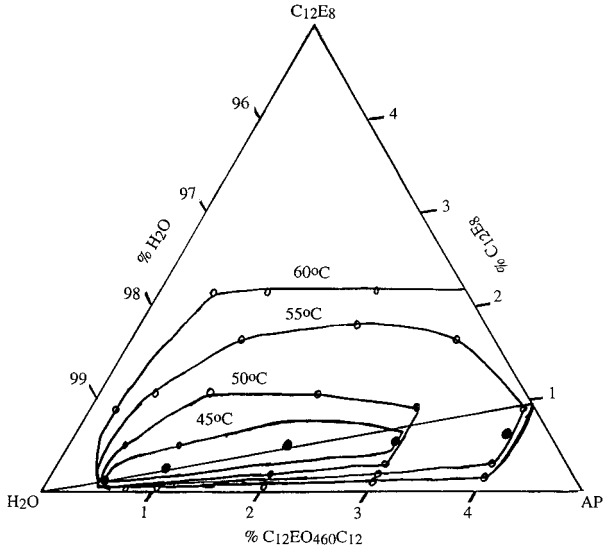

Figure 3. Ternary phase diagram of the $C_{12}E_8$−$C_{12}EO_{460}C_{12}$−water system. The two-phase region is shown at four temperatures: 45, 50, 55, and 60 °C; the line corresponds to the position of the minima in the CPT curve (see Figure 2).

Surfactants interact strongly with hydrophobized polymers and, depending on the properties of the surfactant, they can either favor or hinder phase separation.[33] The variation of the cloud point on addition of surfactant is shown in Figure 2 for several polymer concentrations. With only the polymer present, phase separation results in a dilute and a more concentrated solution, probably containing an extended transient polymer network with hydrophobic nodes. Addition of a nonionic surfactant results in a stabilization of the nodes and the network, so that phase separation occurs at a lower temperature. The increase of the cloud point above a certain surfactant concentration can be understood by dissolution of the network when enough mixed micelles have formed to reduce the number of polymer molecules per node below a critical value. In agreement with this, the surfactant/polymer ratio is practically constant at the cloud point minima, except at the highest polymer concentration.

A schematic ternary phase diagram was determined and is shown at four temperatures in Figure 3. The two-phase region is always situated at low surfactant concentrations and its size increases with temperature. It is well known that the interaction between EO chains

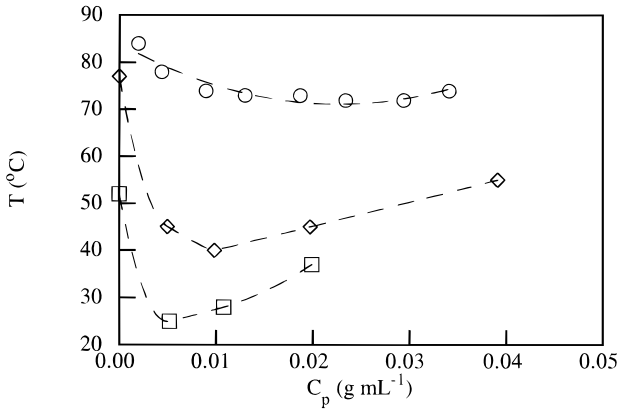

Figure 4. Cloud point temperature of solutions of $C_{12}EO_{460}C_{12}$ (○) and of the mixture of $C_{12}EO_{460}C_{12}$ in the presence of 5 mM of $C_{12}E_8$ (◇) and $C_{12}E_6$ (□).

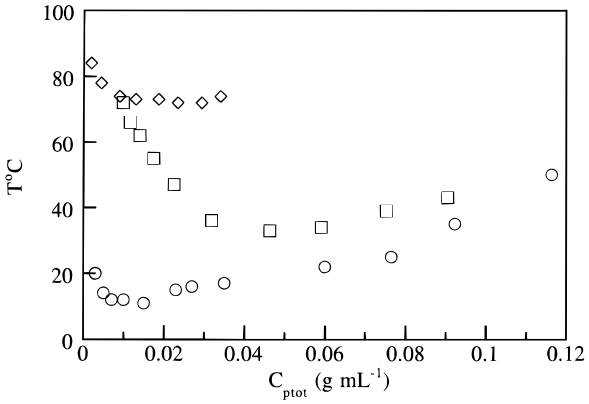

Figure 5. Cloud point temperature of solutions of $C_{12}EO_{460}C_{12}$ (◇), $C_{12}EO_{136}C_{12}$ (○), and the mixture of $C_{12}EO_{136}C_{12}$ with 10^{-2} g mL^{-1} $C_{12}EO_{460}C_{12}$ (□) as a function of the total polymer concentration.

in water becomes more attractive with an increase in temperature. One of several proposed explanations for this is that in the −O−C−C−O sequence there are many nonpolar but only a few polar conformers. Increase in temperature favors the more numerous nonpolar conformers, leading to less favorable water−EO contact.[34] The increased attraction between EO chains results in a larger two-phase area. Reducing the length of the EO chain of the surfactant reduces the hydrophilicity of the surfactant and results in a stronger interaction, as shown in Figure 4 for $C_{12}E_6$. Comparing the phase diagram with that obtained for unmodified PEO, the most important difference is that the two-phase area is an island close to the water corner in the present system, while PEO−C_nE_m gives a segregative phase separation.[35] The $C_{12}EO_{460}C_{12}$−C_nE_m system is of the associative type (*i.e.*, polymer and surfactant are in the same phase).

(b) $C_{12}EO_{460}C_{12}$−$C_{12}EO_{136}C_{12}$ System. The aim of this section is to compare the effect of the triblock copolymer, $C_{12}EO_{136}C_{12}$, on the solubility of $C_{12}EO_{460}C_{12}$ with that of the diblock nonionic surfactant $C_{12}E_8$, as discussed above. Figure 5 shows the cloud point temperature of the mixed system $C_{12}EO_{460}C_{12}$−$C_{12}EO_{136}C_{12}$ as a function of the total concentration, where the concentration of $C_{12}EO_{460}C_{12}$ is held constant (10^{-2} g mL^{-1}). The cloud point curves for the two pure polymers are also shown in the figure. Contrary to the mixed system $C_{12}EO_{460}C_{12}$−$C_{12}E_8$ where the cloud point is dramatically decreased below that of both the polymer and the surfactant, the cloud point of the $C_{12}EO_{460}C_{12}$−$C_{12}EO_{136}C_{12}$ system lies between those of the two pure polymers.

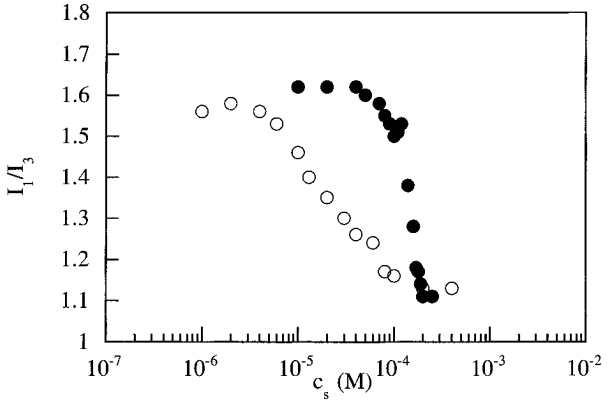

Figure 6. Variation of the intensity ratio I_1/I_3 of the fluorescence pyrene spectrum in aqueous solutions of $C_{12}E_8$ (●) and of $C_{12}E_8$ in mixture with 2.2×10^{-3} g mL^{-1} $C_{12}EO_{460}C_{12}$ (○).

For the mixture of the two polymers, the simple two-state relationship

$$T_{CP}(\text{mix}) = pT^1_{CP} + (1 - p)T^2_{CP} \qquad (8)$$

seems to be valid. Here T_{CP}(mix) is the cloud point of the mixture, T^1_{CP} and T^2_{CP} are the cloud points in the pure polymer solutions, and p is the fraction of polymer 1.

The differences between the polymer−polymer and surfactant−polymer systems show the different roles played by the components in the mixture. In the pure surfactant system, the phase separation at the cloud point is driven by the increasingly attractive interactions between the micelles. Addition of a polymer that strongly associates with the micelles and is able to interconnect them by formation of bridges will, of course, strengthen the attractions and favor phase separation.

The difference between the polymer mixture and the polymer−surfactant system is that when the second polymer is added, it does not have the ability to reinforce the hydrophobic nodes by allowing them to grow from rather small aggregation numbers with a lot of remaining hydrocarbon−water contact to well-developed nonionic micelles. For this to occur, a surfactant with a small hydrophilic group is required.

cac of the Mixed $C_{12}E_8$−$C_{12}EO_{460}C_{12}$ System. The I_1/I_3 ratio of the intensities of the first and third vibronic peaks in the fluorescence spectrum of pyrene was measured in solutions of $C_{12}EO_{460}C_{12}$ (2.2×10^{-3} g mL^{-1}) and $C_{12}E_8$ (Figure 6). These results are compared with those for a pure $C_{12}E_8$ solution.

The ratio I_1/I_3 is an index of the polarity of the probe microenvironment. For pure $C_{12}E_8$ solution, the ratio starts to decrease from 8×10^{-5} M, which corresponds to the cmc. The I_1/I_3 ratio decreases over a rather narrow concentration range and is complete at 2×10^{-4} M, showing that all pyrene is sited in the micelles at this concentration. The I_1/I_3 ratio for the mixed $C_{12}E_8$−$C_{12}EO_{460}C_{12}$ system starts to decrease already at a very low surfactant concentration (6×10^{-6} M), indicating that hydrophobic microdomains start to form at concentrations (cac) much lower than the cmc of the pure surfactant. In this case, the decrease of I_1/I_3 is more gradual, showing a less cooperative aggregation process. All pyrene seems to be in the hydrophobic environment at a surfactant concentration of about 1×10^{-4} M. The total concentration $c_s + c_{eg}$ is then about 3×10^{-4} M.

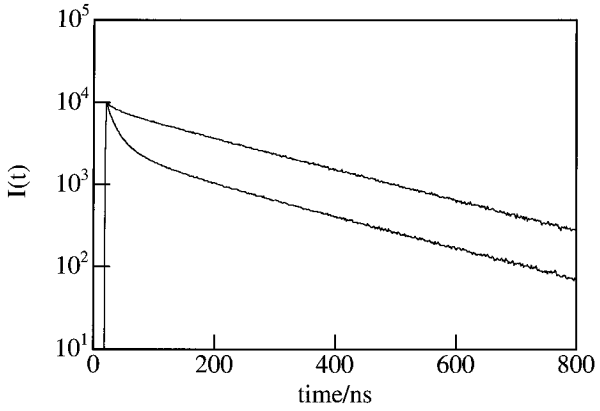

Figure 7. Fluorescence decay curves for pyrene in mixed solutions of $C_{12}E_8$ (5 mM) and $C_{12}EO_{460}C_{12}$ (4×10^{-2} g mL^{-1}) in the absence and presence of quencher.

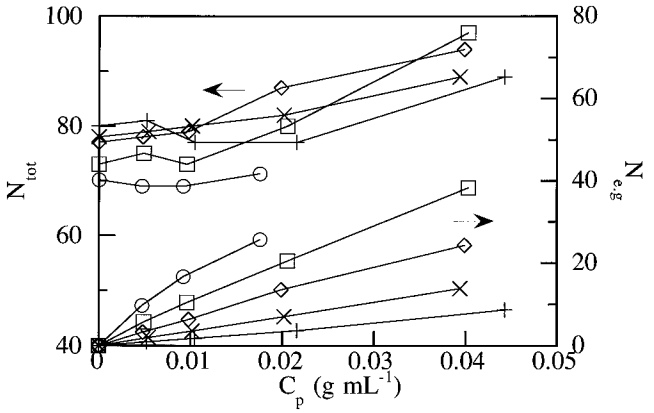

Figure 8. Variation of the total average aggregation number (polymer end groups + surfactant) and the aggregation number of polymer end groups per micelle as a function of the polymer concentration in solutions of 2 (○), 5 (□), 10 (◇), 20 (×) and 40 mM (+) $C_{12}E_8$.

Aggregation Numbers in Mixed Hydrophobic Domains. In this section, we discuss the results from dynamic fluorescence quenching measurements on mixed aggregates of $C_{12}EO_{460}C_{12}$ and $C_{12}E_8$. These results all apply to measurements at 20 °C with polymer concentrations between 0 and 0.04 g mL^{-1}. In the absence of surfactant, the polymer aggregation number is about 15−30 end groups per micelle for $0.01 < C_p < 0.07$ g mL^{-1}.[1] In the presence of the surfactant, the fluorescence decay curves exhibit well-developed tails with decay constants similar to those without quencher (Figure 7), so that eq 1 could be used in the evaluation of the data. As compared to the pure polymer,[1] there is less perturbation from impurity fluorescence at short time scales. The results are of high quality and the values of the aggregation numbers should be reliable. In addition, the cac used in the calculation of the aggregation number is very much lower than the cac for the pure polymer.[1] It is also lower than the cmc of the surfactant $C_{12}E_8$ (cmc: 71 μM). The concentrations of free polymer and surfactant are therefore insignificant in the systems studied (with at least 2 mM $C_{12}E_8$).

The total average aggregation numbers of the hydrophobic domains at different surfactant concentrations are presented as a function of polymer concentration in Figure 8, together with the average number of polymer end groups per domain. We note from these results that there is a slight increase in the micelle aggregation number with surfactant concentration even in the absence of polymer. Up to about 0.02 g mL^{-1} of polymer, the total aggregation numbers change little with polymer concentration, but at the highest polymer concentrations, the numbers increase, to about 95 at 0.04 g mL^{-1}. This is a rather surprising result; looking upon the aggregates as nonionic mixed micelles, one would expect that the introduction of a surfactant with a much larger head group than $C_{12}E_8$ would result in smaller micelles. We have no satisfactory explanation of this effect. It is probably significant, however, that the increase in size occurs at a polymer concentration at which extensive networks should be present in the solution, and the polymer molecules may readily form bridges between the existing micelles, without needing to create new nodes.

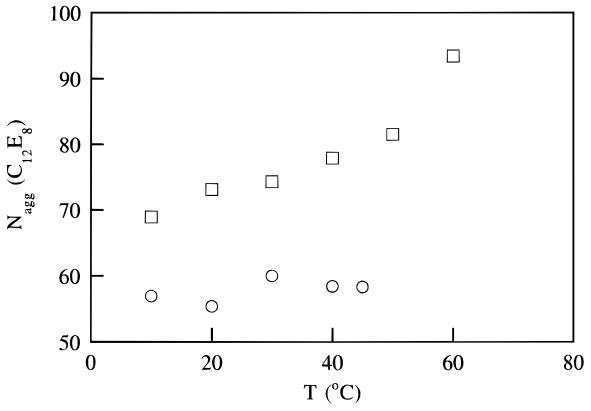

Figure 9. Variation of the aggregation number of $C_{12}E_8$ (c_s = 5 mM) micelles with temperature in water (□) and in a 2×10^{-2} g mL^{-1} solution of $C_{12}EO_{460}C_{12}$ (○).

Figure 8 also shows that the average number of polymer ends per aggregate increases almost in proportion to the polymer concentration, indicating that the number of micelles remains about constant and that the polymer associates with the existing domains, rather than creating new ones. A closer inspection of the data shows that the micelle concentration increases somewhat with polymer concentration at the lowest surfactant concentrations, but not at all at the highest. At 2 mM surfactant, the micelle concentration increases from 0.035 mM without polymer to 0.062 mM at 0.04 g mL^{-1} of the polymer.

The above results pertain to compositions with more surfactant than polymer end groups, and the aggregates are larger than those formed by the polymer end-groups alone, according to our previous estimates.[1] Interestingly, in at least one of the solutions, with 5 mM surfactant and 0.04 g mL^{-1} of polymer, the number of polymers associated with the structure (ca. 20) is larger than in the pure polymer solution. The large hydrophobic domain gives more space for the polymer backbone in the vicinity of the micellar core so that more polymers may associate with it.

Effect of Temperature on $C_{12}E_8$ Aggregation Number. Temperature was found not to influence the aggregation number in contrast to pure nonionic surfactant micelles, where N_{agg} increases strongly from a temperature about 20 °C below the cloud point.[36] Figure 9 shows the variation of the aggregation number of $C_{12}E_8$ as a function of temperature in pure $C_{12}E_8$ (5 mM) solutions and in a mixture with the polymer ($c_{eg} \approx 2$ mM) at the same surfactant concentration. In the absence of polymer, the curve shows the same features already observed with other alkylpoly(oxyethylene glycol monoethers) of the type C_nE_m surfactants.[36,37] Above a certain temperature close to the cloud point, an increase

in N_{agg} is observed. In the presence of the polymer $C_{12}EO_{460}C_{12}$, on the other hand, N_{agg} is constant even near the cloud point of the mixture (ca. 45 °C). As observed by Zana et al.,[38] the micelle aggregation number of nonionic $C_{12}E_8$ does not change in the presence of a low molecular weight unmodified PEO (M_w = 20 000); the behavior was the same as in the absence of polymer. The bulky hydrophobic groups from the polymer in the mixed micelles evidently prevent the formation of larger aggregates, with less curvature. Recent results in the same type of system but a higher M_w PEO (600 000) show that the micelle aggregation number is reduced significantly.[42]

The fact that the aggregation numbers are also independent of temperature allows us to estimate the aggregation numbers for the micelles formed at the compositions which correspond to the minima in the cloud point curves of Figure 2. The surfactant/polymer aggregation numbers are, starting with the lowest concentration of polymer (0.005 g mL^{-1}), 57/5, 60/6, 70/7, and 67/13, giving an almost constant ratio. It will be shown below that a minimum value of the diffusion coefficient as a function of surfactant concentration occurs at about the same composition, whereas the maximum in viscosity requires almost twice as much of the surfactant.

Dynamic Light Scattering Measurements. Dynamic light scattering measurements were made on mixtures of $C_{12}EO_{460}C_{12}$ and the surfactants $C_{12}E_6$, $C_{12}E_8$, and $C_{12}E_{23}$ in dilute aqueous solutions over a wide range of compositions. Mixtures of the two associative polymers, $C_{12}EO_{460}C_{12}$ and $C_{12}EO_{136}C_{12}$, were studied at 25 °C. All measurements were made at a scattering angle of 90°.

(a) $C_{12}EO_{460}C_{12}$−$C_{12}E_8$. 1. Variation of the Diffusion Coefficient of the Aggregates at Fixed $C_{12}E_8$ Concentration. At all polymer concentrations, the measured correlation functions were found to be closely single exponential at high $C_{12}E_8$ concentrations, but double exponential at concentrations below about 1 mM of $C_{12}E_8$. The fact that two modes are present at low surfactant concentration is consistent with observations on the pure polymer without surfactant, where two modes were observed at the same polymer concentration, as discussed previously.[1] At high surfactant concentrations in the present system, the free micelles are not sufficiently different in size from the micelles associated with a single polymer coil to produce separable relaxation modes. We note that the scattered intensity increases strongly on addition of surfactant. This increase (between 3 and 20 times depending on the composition) will be related to the change in mass/contrast between polymer and polymer/surfactant complex.

Figure 10 shows the diffusion coefficients, $D = \Gamma/q^2$, as a function of polymer concentration at 0, 0.6, 1, and 2 mM $C_{12}E_8$. The corresponding relaxation time distributions were bimodal, and the amplitude of the fast mode increases with increasing polymer concentration. Both modes were shown to be diffusive, as determined from the linear dependence of the relaxation rate on the squared scattering vector magnitude. It is clear that the fast diffusion mode, D_f, in this low surfactant concentration region is of the same magnitude independent of the surfactant concentration. In pure polymer solutions, we have previously interpreted the fast diffusion coefficient as originating either from the nonaggregated polymer or from small oligomeric aggregates.[1] On addition of surfactant, the fast mode probably corresponds to mixed micellar aggregates containing a few polymers. The diffusion coefficient of pure $C_{12}E_8$ micelles is about 7×10^{-11} m^2 s^{-1} (see Figure 12), which is close to the value observed at the lowest polymer concentrations. The diffusion coefficient of the pure polymer is about 5×10^{-11} m^2 s^{-1}, and the small mixed aggregates do not diffuse much slower in the concentration range considered. Thus, there seem to exist a population of mixed micelles, as well as the larger clusters of interconnected micelles that give rise to the slow diffusion mode. This slow mode is the dominant feature in the relaxation time distribution already at the lowest concentrations of surfactant and polymer studied (*e.g.*, 0.61 mM $C_{12}E_8$ and 0.1 wt % polymer). In the pure polymer solution, at very low concentration, an even slower mode was noted and attributed to loose complexes formed through PEO−PEO interaction, strengthened by the hydrophobic modification; the fact that this mode disappeared on addition of salt corroborates this interpretation.[1] We conclude that in the surfactant−polymer system the slow mode is due to finite clusters of interconnected mixed micelles.

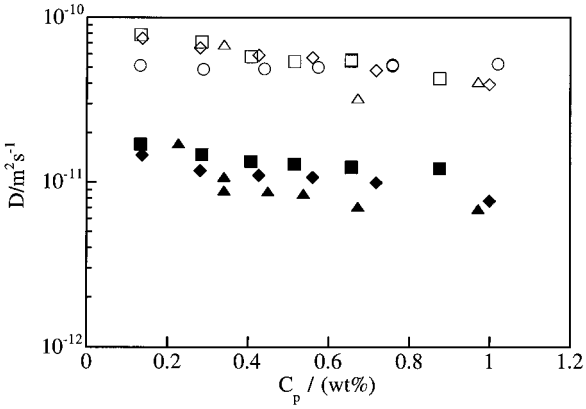

Figure 10. Variation of diffusion coefficient of the fast mode (open symbols) and the slow mode (filled symbols) at different constant $C_{12}E_8$ surfactant concentration (0 (○), 0.61 (□), 0.99 (◇), and 1.88 mM (△)) as a function of polymer content.

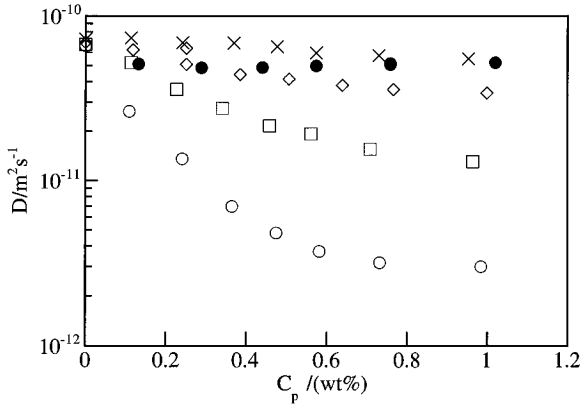

Figure 11. Variation of diffusion coefficient with polymer content at different and constant $C_{12}E_8$ concentration (0 mM fast mode (●), 5 mM (○), 19.3 mM (□), 39.5 mM (◇), and 76.2 mM (×)).

The distributions of the relaxation times at an intermediate surfactant concentration of 5 mM at all polymer concentrations were clearly unimodal. The diffusion coefficients corresponding to this mode are presented in Figure 11 as a function of polymer concentration, at five concentrations of surfactant, and also in the absence

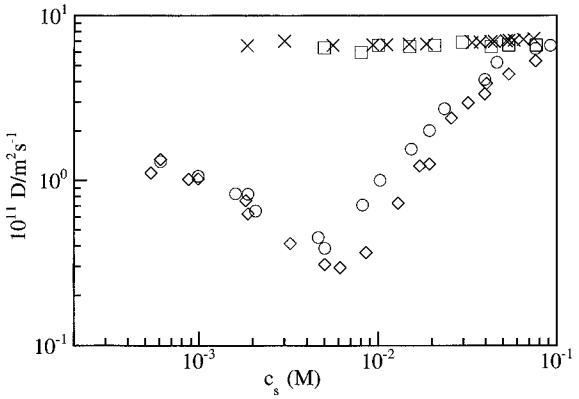

Figure 12. Variation of diffusion coefficient with surfactant concentration at different constant $C_{12}EO_{460}C_{12}$ content [0 (×), 0.5 (○), 1.0 (◇)] and PEO at 0.5 wt % (□).

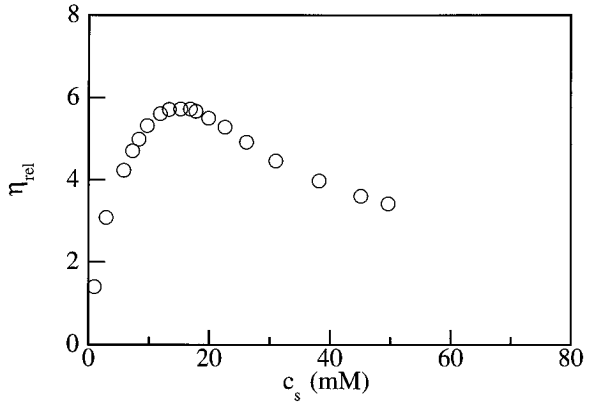

Figure 13. Variation of the relative viscosity of mixed solutions as a function of $C_{12}E_8$ concentration at a constant polymer concentration (9.8×10^{-3} g mL^{-1}).

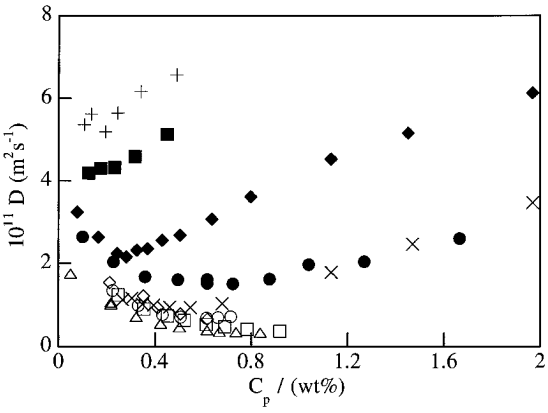

Figure 14. Variation of diffusion coefficient with polymer concentration at different constant $C_{12}E_8/C_{12}EO_{460}C_{12}$ molar ratios: 3 (◇), 4 (□), 9 (△), 16 (○), 20 (×), 30 (●), 47 (◆), 92 (■), and 185 (+).

of surfactant. At the highest surfactant concentrations, 40 and 76 mM, the curves are very similar to the fast mode in Figure 10, but at lower surfactant concentration, the diffusion coefficient decreases strongly with polymer concentration, indicating the formation of multicentered clusters. At the highest polymer concentration, 1 wt %, and 40 mM $C_{12}E_8$, there is less than one polymer per micelle (see Figure 8), and little clustering would be expected, whereas at 5 mM surfactant, there are about 5 polymers per micelle, which would allow the formation of an extensive network. The points for 0.2 wt % polymer, 5 mM surfactant and 1 wt % polymer, 19 mM surfactant correspond to almost the same value of the diffusion coefficient, which is substantially lower than that of the free polymer. From Figure 8 (linear interpolation in the 5 mM case), there would in both cases be an average of about 1.7 polymers per micelle. Evidently, fairly large clusters are already formed under these circumstances.

2. Variation of the Diffusion Coefficient of the Aggregates at Fixed Polymer Concentration. Figure 12 shows D as a function of the concentration of $C_{12}E_8$ at 0, 0.5, and 1 wt % polymer. Apart from the clearly bimodal distribution of the surfactant-free system, the distributions are essentially unimodal. At low surfactant concentration, the diffusion coefficient of the clusters decreases strongly as compared to the values for the unmodified polymer and $C_{12}E_8$.[39] An increase of the diffusion coefficient for the complex is then observed at higher surfactant concentrations and, at the highest concentration, the values approach the curve for the unmodified polymer as well as that for pure $C_{12}E_8$. Here two regions can be clearly distinguished. At low surfactant concentrations, the decrease in D, which shifts slightly toward higher values upon increased polymer concentration, is due to the surfactant-induced formation and stabilization of the network as described above. At high surfactant concentrations, the network dissolves, and free mixed micelles are eventually formed. This type of minimum has been observed with other surfactants and the same type of polymer.[13]

The compositions of the hydrophobic aggregates at the minimum can be estimated from the results in Figure 8. They are found to contain an average of 3−4 polymers per hydrophobic node. The compositions correspond closely to those which give cloud point minima. Evidently, these are compositions which allow extended, probably highly ramified, networks to form, but still, at temperatures below the cloud point, not attractive enough to induce phase separation.

Viscosity Measurements. The relative viscosity of aqueous solutions of $C_{12}EO_{460}C_{12}$ was measured previously.[1] The intrinsic viscosity was found to be lower than that for the unmodified analogue, PEO. In the present study, the relative viscosity of the polymer solutions in the presence of $C_{12}E_8$ has been measured. Figure 13 shows the relative viscosity of the mixed solution at a polymer concentration of 0.98 wt % as a function of surfactant concentration. This curve shows a pronounced maximum of the type already observed in other associative polymer/surfactant systems.[3,13,40,41] The surfactant concentration necessary to produce the viscosity maximum was previously found to depend on the concentration of the associative polymer and its structure. The maximum occurs at a higher surfactant concentration than the minimum observed for the diffusion coefficients and is believed to reflect the formation of larger clusters or a strengthening of the network. From the results in Figure 8, it can be estimated that an average of two polymer molecules is associated with the hydrophobic domains at the composition of the maximum. At higher surfactant concentrations, dissolution of the clusters or network occurs.

3. Variation of the Diffusion Coefficient of the Aggregates at Fixed Molar Ratio (r = $C_{12}E_8$/$C_{12}EO_{460}C_{12}$). The dynamical behavior of the mixed clusters was studied along dilution lines at various ratios, r = number of surfactant molecules/number of polymer end groups. The measured correlation functions are closely single exponential. Results are shown in Figure 14 for the diffusion coefficients as functions

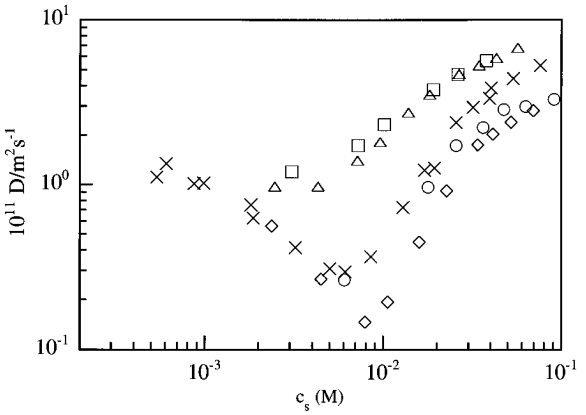

Figure 15. Variation of diffusion coefficients as a function of surfactant concentration at fixed $C_{12}EO_{460}C_{12}$ concentrations; $C_p = 0.5 \times 10^{-2}$ g mL^{-1} for $C_{12}E_6$ (○) and $C_{12}E_{23}$ (□), and $Cp = 10^{-2}$ g mL^{-1} for $C_{12}E_6$ (◇), $C_{12}E_8$ (×), and $C_{12}E_{23}$ (Δ).

of the polymer concentration at various r values. Two regions are clearly present. At high ratios, the diffusion coefficients are high and increase with polymer concentration. The approximate sizes of the aggregates at infinite dilution are about $R_H = 50$ and 40 Å, respectively, for $r = 92$ and $r = 185$. For comparison, R_H for the free $C_{12}E_8$ micelles is about 35 ± 2 Å. Micelles with an average of less than one associated polymer are the diffusing entities in this range of r-values.

At low r-values, on the other hand, and in particular below $r < 20$, the diffusion coefficient decreases strongly with increasing polymer concentration. At intermediate ratios, the diffusion coefficient shows a minimum at a certain concentration, and an increase on dilution. The lowest diffusion coefficients are observed at about the same ratio where the minimum in D is observed as a function of surfactant in Figure 12. It is interesting that an extrapolation to $C_p = 0$ of the single-mode data from higher concentrations, for all curves with r below 47, results in approximately the same value, corresponding to $R_H \approx 140 \pm 20$ Å. The results indicate that multicentered clusters are formed already at very low polymer and surfactant concentrations, since the limiting diffusion coefficient is too small to correspond to surfactant-reinforced flower micelles.

4. Comparison of the Diffusion Coefficient with Three Surfactants at Fixed Polymer Concentration. The diffusion coefficients of the clusters are shown as a function of surfactant concentration in Figure 15 for the three nonionic surfactants, $C_{12}E_6$ and $C_{12}E_{23}$ and $C_{12}E_8$ at concentrations of polymer of 0.005 and 0.01 g mL^{-1}. The results clearly demonstrate that the position and the depth of the minimum, as discussed above, are markedly influenced by the hydrophobicity of the surfactant. In the case of $C_{12}E_6$, the minimum is deeper than for $C_{12}E_8$ and it is shifted toward higher surfactant concentration. For $C_{12}E_{23}$, on the other hand, there is no well-defined minimum in this concentration region. However, if a minimum at low surfactant concentration is present, it is much shallower than for the other two surfactants. The surfactant/end group molar ratio corresponding to the mimima increases for $C_{12}E_{23}$, $C_{12}E_8$, and $C_{12}E_6$, respectively, $r \approx 5$, 7, and 9, with increasing hydrophobicity of the surfactant but is independent of the polymer concentration. A more hydrophobic surfactant is apparently more effective in forming large mixed aggregates.

(b) $C_{12}EO_{460}C_{12}$−$C_{12}EO_{136}C_{12}$. In this section, the dynamic light scattering of mixed aggregates of the two

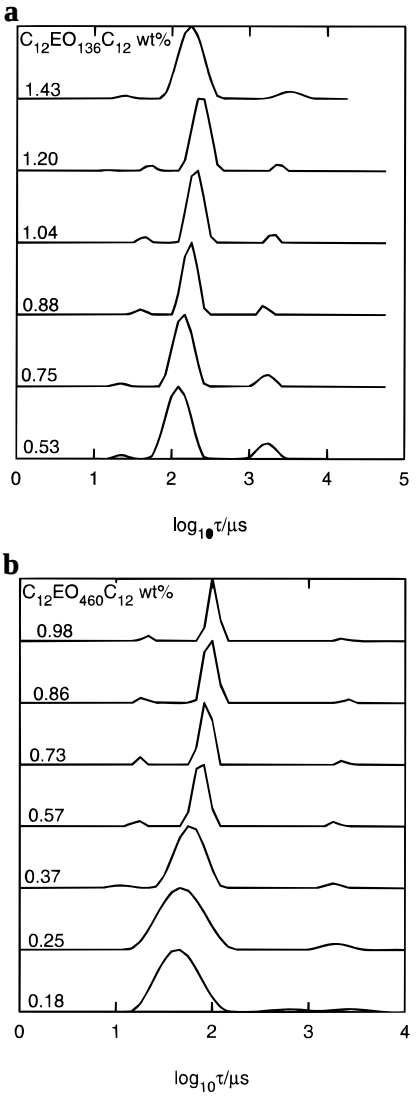

Figure 16. Decay time distributions at various molar ratios ($C_{12}EO_{136}C_{12}/C_{12}EO_{460}C_{12}$): ∞ (a), 0.99 (b).

associative polymers, $C_{12}EO_{460}C_{12}$ and $C_{12}EO_{136}C_{12}$, is considered. As the pure $C_{12}EO_{460}C_{12}$ system has already been investigated,[1] we will start with the results for pure $C_{12}EO_{136}C_{12}$; the measurements were made at 7 °C, which is well below the CPT (Experimental Section). The main difference between these two polymers is that the autocorrelation functions of $C_{12}EO_{136}C_{12}$ are essentially single exponential in the concentration range 0.005−0.014 g mL^{-1} as shown in Figure 16. The relaxation time distributions for this polymer are presented as a function of polymer concentration. The main mode is diffusive and the corresponding diffusion coefficient is plotted in Figure 17.

In Figure 17 the diffusion coefficients are shown as a function of the total concentration of polymer (or polymer end groups). The diffusion coefficients from the fast mode of pure $C_{12}EO_{460}C_{12}$ from ref 1 are also given.

The diffusion coefficients for the mixed system and for the pure short-chain polymer follow the same curve in this representation, and fall between the values for the fast and slow modes of the long-chain polymer. A remarkable feature of the results (not only from DLS) for the latter was the fact that the concentration region with micelle-like aggregates alone is very narrow. A region with unimers or oligomers goes swiftly over into one where multicentered clusters or networks are

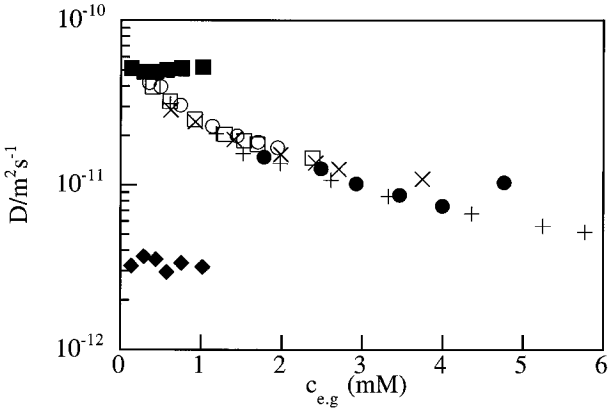

Figure 17. Variation of diffusion coefficients as a function of the total molar polymer end-group concentration at various molar ratios ($C_{12}EO_{136}C_{12}/C_{12}EO_{460}C_{12}$), 0.99 (○), 1.43 (□), 2.82 (×), 5.63 (+), and for pure $C_{12}EO_{460}C_{12}$ (fast mode (■), slow mode (♦)), and pure $C_{12}EO_{136}C_{12}$ (slow mode (●)).

already present together with micelles. At low concentrations a slow mode is present, which represents only a very small fraction of the material and which is strongly suppressed on addition of salt.[1] The aggregates responsible for this slow mode are reminescent of the large aggregates often observed in water-soluble polymers like PEO at low concentrations but are probably reinforced by the more hydrophobic nature of the modified polymer. These aggregates differ from the multicentered clusters appearing at higher concentrations.

In the present case, the diffusion coefficient at low concentrations approaches the value for the fast mode in $C_{12}EO_{460}C_{12}$. As discussed previously,[1] the diffusion coefficient of flower micelles with low aggregation numbers would not be expected to be much lower than that of a unimer; for a micelle with 20 polymers, a fair guess would be a reduction by a factor of 2. The monotonous decrease of the diffusion coefficient must therefore be taken as due to interactions and a progressive clustering of the primary micelles, which for the short-chain polymer start to form at a much lower concentration than for the long-chain compound.

The fact that the diffusion coefficient decreases in the same way with the molar concentration in the mixed systems and in the pure short chain polymer indicates that the concentration of hydrophobic nodes—of similar size—is the decisive factor. This behavior contrasts with that observed when a small nonionic surfactant is added. This is not surprising since the surfactant cannot bridge the micelles and was furthermore shown to have a profound effect on the size of the hydrophobic nodes.

The slow mode appearing at high concentrations of the long-chain polymer corresponds to a much lower diffusion coefficient than that observed for the mixed systems or the short-chain polymer. A direct comparision cannot be made, however, since in the long-chain system the relaxation time distribution is more complex with an additional intermediate mode.

Conclusion

In mixtures of $C_{12}EO_{460}C_{12}$ and the nonionic surfactant, $C_{12}E_8$, hydrophobic microdomains start to form at much lower concentrations than the cac and cmc of the pure systems. The low cac of the mixture promotes formation of larger structures resulting in a depression of the CPT/LCST, below that of both the modified polymer and the surfactant. At higher surfactant additions, however, these structures dissolve and the CPT increases. The phase separation in the pure surfactant system is driven by the increasingly attractive interactions between micelles. The bridges formed by the polymers in the mixed aggregates strengthen these attractions and favor phase separation. A second AP added to an AP solution does not alter the solution structure in the same way. In mixtures of two APs the CPT is found to lie in between those of the two polymers.

Addition of AP to a $C_{12}E_8$ solution slightly increases the total aggregation number of the hydrophobic microdomains, above that of the pure surfactant aggregate. Excluding the very lowest surfactant concentration studied, the added polymer associates with the existing domains rather than forming new ones. As the mixed hydrophobic domains are large, they are able to host more polymer (with bulky head groups) than those of the pure polymer. The bulky hydrophobic groups from the AP in the mixture effectively prevent the increase in N_{agg} generally observed in pure $C_{12}E_8$ systems and also in the presence of unmodified PEO.

The results from the dynamic light scattering and viscosity measurements corroborate the results presented above. At low additions of surfactant to an AP solution, larger structures are formed, resulting in a minimum in diffusion and a maximum in viscosity. The large structures completely dissolve on further surfactant addition. A more hydrophobic surfactant is more effective in forming large mixed aggregates. An AP with shorter PEO chain, $C_{12}EO_{136}C_{12}$, which has a much lower cac than $C_{12}EO_{460}C_{12}$, gives a much simpler relaxation spectrum, and a different concentration dependence. For $C_{12}EO_{136}C_{12}$ alone and in mixtures with the long-chain polymer, the diffusion coefficient decreases in the same way on a molar concentration scale, indicating secondary aggregation which depends on the concentration of hydrophobic nodes.

Acknowledgment. This work has been supported by grants from the Swedish National Board for Industrial and Technical Development (NUTEK). G. Svensk is thanked for viscosity measurements. M. Vasilescu is thanked for static fluorescence measurements. S. Abrahmsén-Alami is aknowledged for stimulating discussions.

References and Notes

(1) Alami, E.; Almgren, M.; Brown, W.; François, J. *Macromolecules* **1996**, *29*, 2229.
(2) Binana-Limbelé, W.; Clouet, F.; François, J. *Colloid Polym. Sci.* **1993**, *271*, 748.
(3) Binana-Limbelé, W.; Clouet, F.; François, J. Unpublished results.
(4) Richey, B.; Kirk, A. B.; Eisenhart, E. K.; Fitzwater, S.; Hook, J. *J. Coat. Technol.* **1991**, *63*, 31.
(5) Lindblad, C.; Almgren, M.; Persson, K.; Abrahmsén-Alami, S.; Stilbs, P. Unpublished results.
(6) *Hydrophilic Polymers*; Alami, E., Rawiso, M., Isel, F., Beinert, G., Binana-Limbele, W., François, J., Eds.; Advances in Chemistry 248; American Chemical Society: Washington, DC, 1996.
(7) Maechling-Strasser, C.; François, J.; Clouet, F.; Tripette, C. *Polymer* **1992**, *33*, 627.
(8) Maechling-Strasser, C.; Clouet, F.; François, J. *Polymer* **1992**, *33*, 1021.
(9) Nyström, B.; Walderhaug, H.; Hansen, F. K. *J. Phys. Chem.* **1993**, *97*, 7743.
(10) Persson, K.; Abrahmsén, S.; Stilbs, P.; Walderhaug, H.; Hansen, F. K. *Colloid Polym. Sci.* **1992**, *270*, 465.
(11) Walderhaug, H.; Hansen, F. K.; Abrahmsén, S.; Persson, K.; Stilbs, P. *J. Phys. Chem.* **1993**, *97*, 8336.
(12) Abrahmsén-Alami, S.; Stilbs, P. *J. Phys. Chem.* **1994**, *98*, 6359.

(13) Persson, K.; Wang, G.; Olofsson, G. *J. Chem. Soc., Faraday Trans* **1994**, *90* (23), 3555.
(14) Persson, K.; Bales, B. L. *J. Chem. Soc., Faraday Trans.* **1995**, *91* (17), 2863.
(15) Abrahmsén-Alami, S.; Alami, E.; François, J. *Colloid Interface Sci.* **1996**, *179*, 20−33.
(16) Jenkins, R. D. Ph.D. Dissertation, Lehigh University, Bethlehem, PA, 1990.
(17) *The Function of Associative Thickeners in Water-borne Paints*; Huldén, M.; Sjöblom, E.; Boström, P.; XXI FATIPEC Congress, Amsterdam, 1992.
(18) Huldén, M. *Colloids Surf. A* **1994**, *82*, 263.
(19) Goddard, E. D. *Colloids Surf.* **1986**, *19*, 255.
(20) *Nonionic Surfactants*; Saito, S., Physical Chemistry. In Schick, M. J., Ed.; Surfactants Series 23, 1987, pp 881−925.
(21) *Physics of Amphiphiles: Micelles, Vesicles and Microemulsions*; Degiorgio, V.; Corti, M.; International School of Physics (ENRICO FERMI), 1985, pp 303−335.
(22) Corti, M.; Minero, C.; Degiorgio, V. *J. Phys. Chem.* **1984**, *88*, 309.
(23) Woodhead, J. L.; Lewis, J. A.; Malcom, G. N.; Watson, I. D. *J. Colloid Interface Sci.* **1981**, *79*, 554.
(24) Kalyanasundaram, K.; Thomas, J. K. *J. Am. Chem. Soc.* **1977**, *99*, 2039.
(25) Almgren, M.; Hansson, P.; Mukhtar, E.; Van Stam, J. *Langmuir* **1992**, *8*, 2405.
(26) Infelta, P. P.; Grätzel, M.; Thomas, J. K. *J. Phys. Chem.* **1974**, *78*, 190.
(27) Tachiya, M. *Chem. Phys. Lett.* **1975**, *33*, 289.
(28) Infelta, P. P. *Chem. Phys. Lett.* **1979**, *61*, 88.
(29) Atik, S. S.; Nam, M.; Singer, L. A. *Chem. Phys. Lett.* **1979**, *67*, 75.
(30) Brown, W.; Schillén, K.; Almgren, M.; Hvidt, S.; Bahadur, P. *J. Phys. Chem.* **1991**, *95*, 1850.
(31) (a) Jakes, J. *Czech J. Phys.* **1988**, *B38*, 1305. (b) Johnsen, R. M.; Brown, W. *Laser Light Scattering in Biochemistry*; Harding, S. E., Sattelle, D. B., Bloomfield, V. A., Eds.; Royal Society of Chemistry: London, 1992; p 77.
(32) Saeki, S.; Kuwahara, N.; Nakata, N.; Kaneko, M. *Polymer* **1976**, *17*, 685.
(33) Piculell, L.; Lindman, B. *Adv. Colloid Interface Sci.* **1992**, *41*, 149−179.
(34) Karlström, G. *J. Phys. Chem.* **1985**, *89*, 4962.
(35) Piculell, L.; Bergfeldt, K.; Gerdes, S. Submitted to *J. Phys. Chem.*
(36) Binana-Limbelé, W.; Zana, R. *J. Colloid. Interface Sci.* **1988**, *121*, 111.
(37) Alami, E.; Kamenka, N.; Raharimihamina, A.; Zana, R. *J. Colloid Interface Sci.* **1993**, *158*, 342.
(38) Anthony, O.; Zana, R. *Langmuir* **1994**, *10*, 4048.
(39) Feitosa, E.; Brown, W.; Hansson, P. *Macromolecules* **1996**, *29*, 2169.
(40) Kaczmarski, J. P.; Glass, J. E. *Macromolecules* **1993**, *26*, 5149.
(41) Lundberg, D. J.; Brown, R. G.; Glass, J. E.; Eley, R. R. *Langmuir* **1994**, *10*, 3027.
(42) Feitosa, E.; Brown, W.; Swanson-Vethamuthu, M. Submitted to *J. Phys. Chem.*

MA9518161